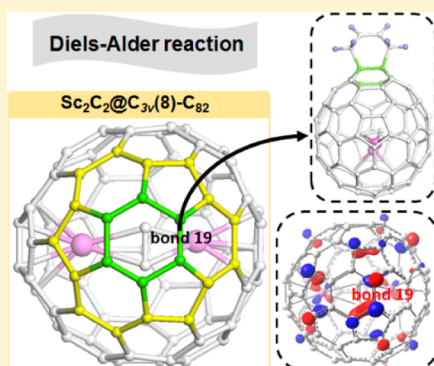


Regioselectivity of $\text{Sc}_2\text{C}_2@C_{3v}(8)\text{-C}_{82}$: Role of the Sumanene-Type Hexagon in Diels–Alder Reaction

Pei Zhao,[†] Xiang Zhao,^{*,†} and Masahiro Ehara[‡][†]Institute for Chemical Physics & Department of Chemistry, State Key Laboratory of Electrical Insulation and Power Equipment, School of Science, Xi'an Jiaotong University, Xi'an 710049, China[‡]Institute for Molecular Science, Okazaki 444-8585, Japan

Supporting Information

ABSTRACT: Recently, several experiments have demonstrated high chemical reactivity of the sumanene-type hexagon in $\text{Sc}_2\text{C}_2@C_{82}$. To further uncover its reactivity, the Diels–Alder reaction to all the nonequivalent C–C bonds of C_{82} and $\text{Sc}_2\text{C}_2@C_{82}$ has been investigated by density functional theory calculations. For the free fullerene, the [5,6] bond 7 is the thermodynamically most favored, whereas the addition on the [6,6] bond 3 has the lowest activation energy. Diels–Alder reaction has no preference for addition sites in the sumanene-type hexagon. However, in the case of the endohedral fullerene, the [6,6] bond 19 in the special hexagon becomes the most reactive site according to both kinetic and thermodynamic considerations. Further analyses reveal that bond 19 in $\text{Sc}_2\text{C}_2@C_{82}$ exhibits the shortest bond length and third largest π -orbital axis vector. In addition, the LUMOs of bond 19 are also symmetry-allowed to interact with butadiene.



INTRODUCTION

Endohedral metallofullerenes (EMFs) have attracted broad attention due to their novel structures, fascinating properties, and potential applications in fields such as materials science or medicinal chemistry.^{1–6} Furthermore, chemical modification of EMFs is useful to facilitate their structural characterization and tune their physical and chemical properties for future applications.^{1,5,7–16}

Until now, many investigations have been carried out to functionalize EMFs and to get a better understanding of their reactivity. Nevertheless, the chemical functionalization of EMFs mainly focused on EMFs with high yields (e.g., $\text{La}@C_{82}$ and $\text{Sc}_3\text{N}@C_{80}$).^{12,17–23} Few reactivity studies have been devoted to carbide clusterfullerenes, and the purpose for their functionalization is often to facilitate the growth of single crystals by the corresponding derivatives.²⁴ Solà et al. investigated the influence of metal clusters in the Diels–Alder (DA) reaction of C_{80} and its EMF derivatives including $\text{Sc}_3\text{C}_2@C_{80}$ and $\text{Sc}_4\text{C}_2@C_{80}$, and they pointed out that the combination of four parameters (the metallic cluster size, the transferred charge, the HOMO–LUMO gap of the compound, and the deformation of EMFs) is important to understand and explain their reactivity and regioselectivity.²⁵ Later, the same group disclosed the higher reactivity of $\text{Ti}_2\text{C}_2@D_{3h}\text{-C}_{78}$ compared to that of $\text{M}_3\text{N}@D_{3h}\text{-C}_{78}$ ($\text{M} = \text{Sc}, \text{Y}$) through theoretical investigations of DA reaction for both endohedral and free fullerenes.^{26–28}

As the prototype of carbide clusterfullerenes, chemical modification of $\text{Sc}_2\text{C}_2@C_{3v}(8)\text{-C}_{82}$ has been explored by several groups. To determine the structure of $\text{Sc}_2\text{C}_2@C_{3v}(8)\text{-C}_{82}$, its carbene derivative was identified by single-crystal analysis, and an opened structure was obtained by the [5,6] addition of Ad

(hereafter the label of isomer $C_{3v}(8)$ is omitted for clarity).²⁹ Later, a complexation with a Re_3 cluster was synthesized, and the Re_3 triangle was positioned over three [6,6] junctions of a hexagon.³⁰ Meanwhile, it has been found that the hexagon is far away from the encapsulated cluster and surrounded by three hexagons and three pentagons (named sumanene; see Figure 1), which results in higher ring strain and less conjugation energy than the other hexagons (surrounded by four or five hexagons). A subsequent report also revealed the preference of a metal triangle to bind sumanene-type hexagons.³¹ Very recently, 1,3-dipolar reaction of $\text{Sc}_2\text{C}_2@C_{82}$ was successfully performed in experiment, and the single-crystal structure of the major adduct confirmed the addition on a [6,6] junction.³² Interestingly, although those additions may not occur at the same bond of $\text{Sc}_2\text{C}_2@C_{82}$, those preferred addition junctions locate at the same hexagon, that is, the sumanene-type hexagon. Cai and co-workers pointed out that highly concentrated area of reactivity should be attributed to the overlap of high π -orbital axis vector (POAV) angles and large LUMO coefficients.³² However, is there any other factor influencing chemical reactivity on the special hexagon? Does the special hexagon also show high chemical activity in other reactions? Further investigations are necessary to answer those questions.

Herein, a systematic theoretical study of the DA reaction on both C_{82} and $\text{Sc}_2\text{C}_2@C_{82}$ has been performed by density functional theory calculations. Both thermodynamics and kinetics have been taken into account to uncover the impact of the special hexagon and the Sc_2C_2 unit on the reaction

Received: April 26, 2016

Published: August 18, 2016



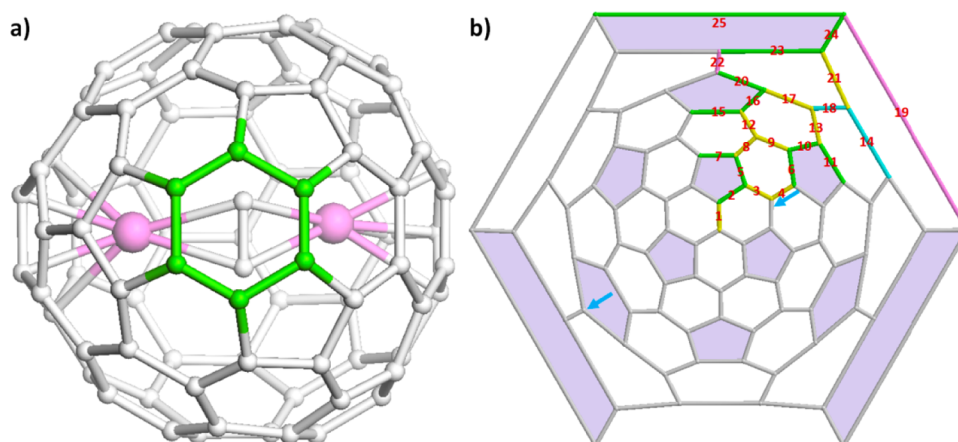


Figure 1. (a) Molecular structure of $\text{Sc}_2\text{C}_2@C_{3v}(8)\text{-C}_{82}$ (top view), in which the sumanene-type hexagon is colored green. (b) Schlegel diagram of $C_{3v}(8)\text{-C}_{82}$, in which 25 nonequivalent C–C bonds are denoted with Arabic numerals and highlighted by four different colors (that is, the four bond types). It should be noted that the most external six-membered ring is the ring colored in green in (a), and the positions of two Sc atoms are marked by two blue arrows.

mechanisms and chemical selectivity. In addition, the origin of the regioselectivity was also discussed.

COMPUTATIONAL METHODS

Full geometry optimizations on all relevant structures [reactants, transition states, and products] were carried out at the level of M06-2X/6-31G(d)~Lan12dz^{33,34} (the 6-31G(d) basis set was used for H and C, and the Lan12dz basis set with the corresponding effective core potential was used for Sc).^{35–37} Based on the optimized structures, vibrational analyses were conducted to verify the stationary points to be minima or saddle points on the potential energy surface. In addition, intrinsic reaction coordinate analyses on some transition states were performed.^{38–40} The Gaussian 09 program was employed throughout this work.⁴¹

RESULTS AND DISCUSSION

Diels–Alder Reaction of 1,3-Butadiene with C_{82} and $\text{Sc}_2\text{C}_2@C_{82}$. As shown in Figure 1, the C_{3v} -symmetric C_{82} cage contains a total of 25 nonequivalent C–C bonds including four bond types (A, B, C, and D; see Figure S1 in the Supporting Information).⁴² Compared to the pristine carbon cage, $\text{Sc}_2\text{C}_2@C_{82}$ possesses the C_s symmetry for preferential orientation of the metallic cluster, thus, 66 nonequivalent C–C bonds can be figured out. Due to the rotation of the Sc_2C_2 unit, only 25 distinct adducts could be generated in the DA reaction. However, it is not simple to investigate the cycloaddition reaction by computational methods. Several studies have pointed out that rotation of the cluster inside a functionalized cage is more hindered than that in a pristine EMF.^{25,43,44} Consequently, 66 nonequivalent C–C bonds of $\text{Sc}_2\text{C}_2@C_{82}$ have been considered to determine the lowest-energy orientations for 25 different adducts (see Table S1 in the Supporting Information).

First, as shown in Table 1, reaction energies of additions on all the nonequivalent C–C bonds of C_{82} and $\text{Sc}_2\text{C}_2@C_{82}$ have been predicted. For the free fullerene, generally, the reaction is more favored over [5,6] bonds than over [6,6] bonds, which coincides with reaction energies of C_{68} and C_{78} in DA reactions.^{26,45} For example, the three most exothermic reactions were found for [5,6]-type D bonds, that is, bond 7 ($-47.1 \text{ kcal}\cdot\text{mol}^{-1}$), bond 5 ($-46.8 \text{ kcal}\cdot\text{mol}^{-1}$), and bond 2 ($-46.3 \text{ kcal}\cdot\text{mol}^{-1}$). The least exothermic addition is obtained for the [6,6]-type C bond 18 ($4.0 \text{ kcal}\cdot\text{mol}^{-1}$). Obviously, for

Table 1. Reaction Energies (ΔE_r) and Energy Barriers (ΔE^\ddagger) Relative to Reactants for DA Reaction of C_{82} and $\text{Sc}_2\text{C}_2@C_{82}$ at the M06-2X/6-31G*~Lan12dz Level of Theory (Values Are Given in $\text{kcal}\cdot\text{mol}^{-1}$)

bond	bond type	C_{82}		$\text{Sc}_2\text{C}_2@C_{82}$	
		ΔE_r	ΔE^\ddagger	ΔE_r	ΔE^\ddagger
1	B[6,6]	-21.6	17.1	-12.2	24.0
2	D[5,6]	-46.3	3.5	-23.4	21.9
3	B[6,6]	-24.3	2.6	-18.6	22.7
4	B[6,6]	-21.5	4.8	-14.0	24.5
5	D[5,6]	-46.8	5.8	-25.7	17.9
6	D[5,6]	-42.8	3.5	-24.5	19.5
7	D[5,6]	-47.1	5.4	-27.8	16.2
8	B[6,6]	-28.1	4.1	-11.8	23.5
9	B[6,6]	-18.4	12.3	-14.7	22.5
10	D[5,6]	-38.4	9.9	-20.1	22.3
11	D[5,6]	-36.0	13.4	-20.5	20.2
12	B[6,6]	-19.6	4.2	-19.3	19.4
13	B[6,6]	-27.3	8.5	-14.0	21.1
14	C[6,6]	-4.2	25.5	1.7	28.9
15	D[5,6]	-34.4	10.2	-21.7	20.0
16	D[5,6]	-45.0	5.4	-25.4	21.4
17	B[6,6]	-24.7	11.6	-23.5	18.7
18	C[6,6]	4.0	11.3	-2.5	28.6
19	A[6,6]	-30.1	10.7	-32.2	10.7
20	D[5,6]	-17.9	10.8	-15.1	20.9
21	B[6,6]	-28.1	11.4	-19.1	17.1
22	A[6,6]	-30.1	10.8	-19.3	18.0
23	D[5,6]	-17.6	20.2	-24.4	18.8
24	D[5,6]	-25.9	16.3	-17.5	21.9
25	D[5,6]	-3.6	26.8	-5.8	27.0

the four types of bonds mentioned above, most type D bonds exhibit more negative reaction energies than other bonds. However, for two nonequivalent C–C bonds in the only sumanene-type hexagon, reaction energies are -30.1 and $-3.6 \text{ kcal}\cdot\text{mol}^{-1}$ for bonds 19 and 25, respectively. It should be noted that the reaction on bond 25 of the special hexagon is the least exothermic one among all of the type D bonds considered. Meanwhile, another type A bond 22 exhibits the same reaction energy with bond 19.

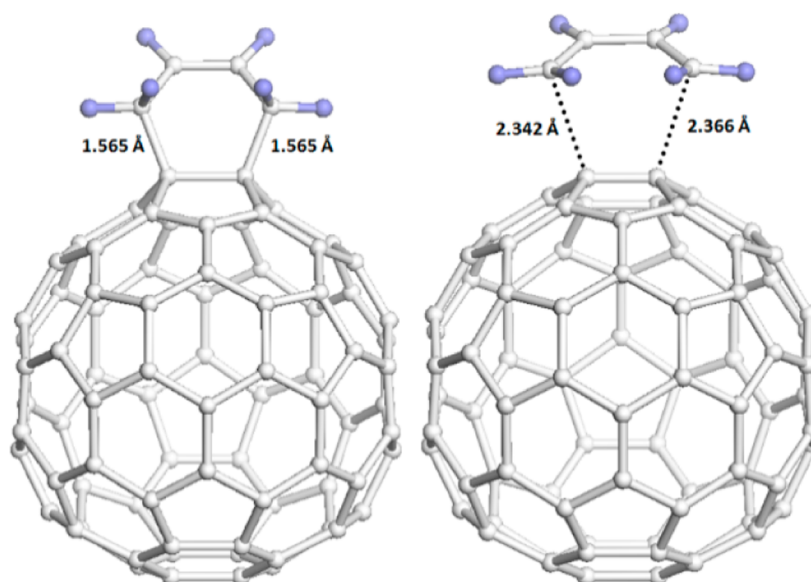


Figure 2. Optimized geometries of product (left) and TS (right) from bond 7 in C_{82} .

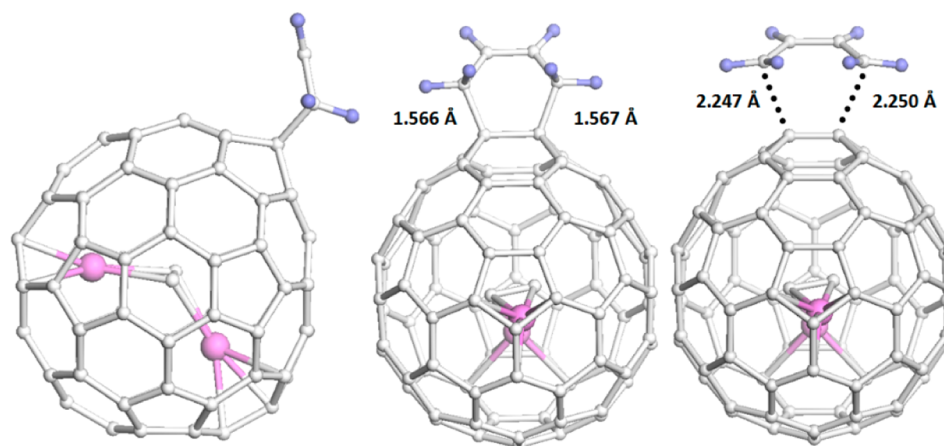


Figure 3. Optimized geometries of product (left, side view; middle, front view) and TS (right) from bond 19 in $Sc_2C_2@C_{82}$.

When the Sc_2C_2 cluster is trapped into C_{82} , the reaction energies for most C–C bonds are reduced dramatically, which is similar to previous studies.^{26,45} Interestingly, the most exothermic reaction (bond 7, $-47.1 \text{ kcal}\cdot\text{mol}^{-1}$) in C_{82} turns out to be the second most exothermic one ($-27.8 \text{ kcal}\cdot\text{mol}^{-1}$) in $Sc_2C_2@C_{82}$. The most exothermic reaction is found for type A bond 19 of the sumanene-type hexagon ($-32.2 \text{ kcal}\cdot\text{mol}^{-1}$), which is even more exothermic than that on the same bond of the free fullerene. However, the reaction energy of the type A bond 22 decreased to $-19.3 \text{ kcal}\cdot\text{mol}^{-1}$ due to the influence of Sc_2C_2 cluster. For the other bond of the special hexagon, the reaction energy on bond 25 is slightly negative ($-5.8 \text{ kcal}\cdot\text{mol}^{-1}$) after the Sc_2C_2 cluster is encapsulated, but it is still unfavorable for the reaction. The most endothermic addition (bond 18, $4 \text{ kcal}\cdot\text{mol}^{-1}$) in C_{82} generates a negative reaction energy ($-2.5 \text{ kcal}\cdot\text{mol}^{-1}$) in $Sc_2C_2@C_{82}$. Thus, the addition on type C bond 14 becomes the most endothermic one ($1.7 \text{ kcal}\cdot\text{mol}^{-1}$) in the endohedral fullerene. The adduct between 1,3-butadiene and bond 19 is shown in Figure 2, in which the orientation of the Sc_2C_2 cluster coincides with that in the original $Sc_2C_2@C_{82}$ (see Figure S2 in the Supporting Information).

Then, as presented in Table 1, all the transition states (TSs) in the above DA reactions of C_{82} and $Sc_2C_2@C_{82}$ were investigated to evaluate their energy barriers. For C_{82} , the three most exothermic products (additions on bonds 7, 5, and 2) have the lower energy barriers, but they are not the lowest ones. The lowest barrier ($2.6 \text{ kcal}\cdot\text{mol}^{-1}$) is found for bond 3, which possesses a smaller reaction energy ($-24.3 \text{ kcal}\cdot\text{mol}^{-1}$). The activation energies are 5.4, 5.8, and $3.5 \text{ kcal}\cdot\text{mol}^{-1}$ for bonds 7, 5, and 2, respectively. As a result, the reaction on bond 7 is thermodynamically preferred, whereas the reaction on bond 3 is kinetically preferred, and this suggests that the thermodynamic and kinetic products do not always correspond to the same product. The energy barriers of two nonequivalent bonds in the sumanene-type hexagon are 10.7 and $26.8 \text{ kcal}\cdot\text{mol}^{-1}$ for bonds 19 and 25, respectively. The type A bond 22 still generates the comparable energy barrier ($10.8 \text{ kcal}\cdot\text{mol}^{-1}$) compared with bond 19. The product and TS of the DA reaction of 1,3-butadiene with bond 7 are presented in Figure 2.

In the case of $Sc_2C_2@C_{82}$, most reactions have higher energy barriers with respect to the corresponding reactions in C_{82} . Therefore, from both thermodynamic and kinetic viewpoints, the encapsulation of the cluster reduces the exohedral reactivity of the fullerene surface. The addition on bond 19, which leads

to the thermodynamic control product, is also the kinetically most favorable (energy barrier of 10.7 kcal·mol⁻¹). It should be noted that the energy barrier of bond 19 in Sc₂C₂@C₈₂ is the same as that in C₈₂. Bond 25 of the sumanene-type hexagon also has a similar energy barrier of 27.0 kcal·mol⁻¹ compared to that in C₈₂. On the contrary, the reaction on the type A bond 22 in Sc₂C₂@C₈₂ has a higher energy barrier (18.0 kcal·mol⁻¹) than that in the free fullerene. As mentioned above, the special hexagon is far away from the encapsulated cluster, which may lead to the little difference in reaction and activation energies between the free and endohedral fullerene. The second lowest energy barrier is 16.2 kcal·mol⁻¹ for bond 7. Other TSs are found at considerably higher energies (17.1–28.9 kcal·mol⁻¹). Overall, the addition on bond 19 for the DA reaction between Sc₂C₂@C₈₂ and 1,3-butadiene is the most favorable under thermodynamic and kinetic conditions. Figure 3 depicts the TS of 1,3-butadiene with bond 19, and an almost symmetric structure was located.

Origin of the Regioselectivity. In order to rationalize the chemical reactivity of C₈₂ and Sc₂C₂@C₈₂, especially the sumanene-type hexagon, bond lengths and local strain of all the nonequivalent bonds were investigated first. The POAV angle is common to estimate the atomic local strain in the molecule.⁴⁶ Short C–C bonds with large POAV values not only possess more double-bond character but also are able to bond with other atoms to release strain; thus, those bonds should be preferable in DA reactions.⁴⁵ As shown in Table 2, the obvious changes in bond lengths and POAVs induced by the encapsulation of the Sc₂C₂ cluster are found in the bonds close to the scandium ions (bond 4 and 6), which is consistent

Table 2. POAV Values (in deg) and Bond Lengths (R_{cc} , in Å) for All Nonequivalent Bonds in C₈₂ and Sc₂C₂@C₈₂

bond	bond type	C ₈₂		Sc ₂ C ₂ @C ₈₂	
		R_{cc}	POAV ^a	R_{cc}	POAV ^a
1	B[6,6]	1.417	9.28	1.423	9.93
2	D[5,6]	1.467	10.31	1.429	10.48
3	B[6,6]	1.436	9.69	1.420	9.87
4	B[6,6]	1.400	9.87	1.464	12.54
5	D[5,6]	1.393	10.51	1.431	9.99
6	D[5,6]	1.443	10.71	1.458	11.86
7	D[5,6]	1.465	10.60	1.419	10.65
8	B[6,6]	1.436	9.87	1.432	9.82
9	B[6,6]	1.413	9.89	1.426	9.57
10	D[5,6]	1.429	10.17	1.432	8.91
11	D[5,6]	1.450	9.77	1.420	10.10
12	B[6,6]	1.412	9.90	1.408	9.71
13	B[6,6]	1.404	9.00	1.408	8.61
14	C[6,6]	1.459	7.67	1.463	7.55
15	D[5,6]	1.471	10.43	1.436	10.47
16	D[5,6]	1.410	10.90	1.451	11.45
17	B[6,6]	1.428	9.72	1.405	9.50
18	C[6,6]	1.468	7.96	1.461	7.43
19	A[6,6]	1.378	11.41	1.371	11.62
20	D[5,6]	1.444	10.99	1.430	10.88
21	B[6,6]	1.414	9.14	1.417	9.13
22	A[6,6]	1.360	10.77	1.371	10.75
23	D[5,6]	1.452	10.32	1.437	10.95
24	D[5,6]	1.423	11.00	1.433	11.10
25	D[5,6]	1.462	11.44	1.455	11.47

^aAverage of the two POAV values of two carbon atoms involved.

with previous reports.^{26,32} In particular, the bond length and POAV of bond 4 increase significantly with respect to the free fullerene. However, the combination of the two factors cannot make the reaction more reactive. Both bond lengths and POAV values of bonds in C₈₂ and Sc₂C₂@C₈₂ are discussed below.

The bond distance is not always effective to predict the chemical reactivity sequence. For C₈₂, even though bonds 19 and 22 have the two shortest bond lengths (1.378 and 1.360 Å, respectively), they are not the most favorable products based on the reaction energies and activation energies. On the contrary, the most exothermic bond 7 possesses the longer bond length (1.465 Å). In the case of Sc₂C₂@C₈₂, both bonds 19 and 22 possess the shortest bond length (1.371 Å), but the most exothermic reaction is only found for bond 19. The reactivity trend of other bonds does not coincide with the predicted order based on the bond length, either. Compared to bond length, the local molecular strain is more widely used to estimate reactivity of fullerenes. For C₈₂, the five most exothermic bonds (7, 5, 2, 16, and 6) exhibit larger POAVs (10.31–10.90°). The large endothermicity of bond 18 concurs well with its low POAV (7.96°). However, for the sumanene-type hexagon, bonds 19 and 25 with the two largest POAVs provide modest exothermic products. In the case of Sc₂C₂@C₈₂, the most reactive bond 19 possesses the third largest POAV (11.62°) after two bonds close to the Sc ions. The two most endothermic bonds 14 and 18 have the lowest POAVs (7.55 and 7.43° for bond 14 and bond 18, respectively). Apparently, the most reactive bond 19 for the DA reaction in Sc₂C₂@C₈₂ possesses the shortest bond separation and third largest POAV.

The molecular orbitals of C₈₂ and Sc₂C₂@C₈₂ were investigated to understand the reactivity of those C–C bonds. For DA reactions of fullerenes, it is well accepted that the major orbital interaction happens between the HOMO of butadiene and LUMOs of the fullerene. In addition, the energy level difference between the HOMO of 1,3-butadiene (–7.64 eV) and LUMOs of fullerenes can affect the chemical reactivity; that is, the smaller LUMO_{fullerene}–HOMO_{butadiene} gap leads to the higher reactivity of fullerenes. Figure 4 depicts several LUMOs of C₈₂ and Sc₂C₂@C₈₂. It is apparent that the energy levels of LUMOs in the endohedral fullerene (–2.88 and –2.76 eV for LUMO and LUMO+1) are higher than those in the free fullerene (–4.25 and –3.87 eV for LUMO and LUMO+1), which could result in the lower reactivity compared to that with the free fullerene. For the free fullerene, there is no LUMO or LUMO+1 orbital distribution on the sumanene-type hexagon, while marked contributions of LUMO+2 and LUMO+3 could be found for carbon atoms of the special hexagon. The energy level of LUMO+3 is only 0.10 eV higher than that of LUMO+2. What's more, based on Woodward–Hoffmann rule⁴⁷ and frontier orbital theory,⁴⁸ when LUMOs of C–C bonds possess symmetry-allowed shapes and obvious distribution, the corresponding bonds present better reactivity in the cycloaddition reaction. The adequate shape of LUMO+2 or LUMO+3 is found for bond 19, whereas the symmetry-unallowed shape of LUMO+2 or LUMO+3 is found for bond 25. Consequently, it is reasonable that the addition on bond 19 is more favorable than that on bond 25. In addition, several bonds of C₈₂, including bonds 5, 7, 8, 17, 21, 22, and 24, have proper LUMOs to interplay with the HOMO of butadiene, but only bonds 5 and 7 have high reactivity.

For the endohedral fullerene, it should be noted that the orbital distributions on LUMO and LUMO+1 of Sc₂C₂@C₈₂

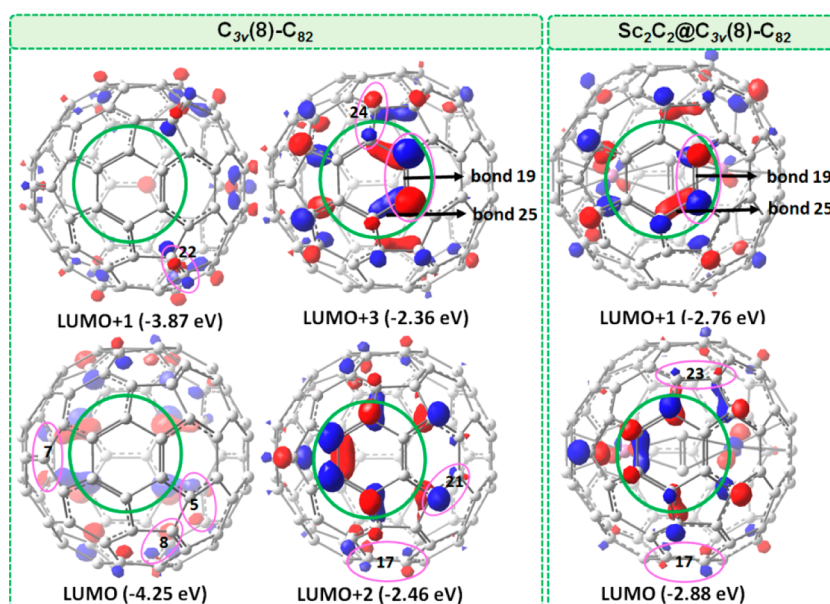


Figure 4. Representation of LUMOs of C_{82} and $Sc_2C_2@C_{82}$ (isosurface values are 0.05), in which the sumanene-type hexagon is circled with green. Those C–C bonds with proper LUMOs to interplay with the HOMO of butadiene are circled with pink.

are similar to those on LUMO+2 and LUMO+3 of C_{82} , respectively. The energy level difference between LUMO+1 and LUMO in $Sc_2C_2@C_{82}$ is also rather small (0.12 eV). This situation should be attributed to the transfer of four electrons from the metallic cluster to the carbon cage. Thus, the most reactive bond 19 possesses the suitable LUMOs to interact with the HOMO of butadiene. The LUMOs of the [5,6] bond 25 in the sumanene-type hexagon are still symmetry-unallowed with butadiene, which concurs well with the low reactivity of bond 25 in the DA reaction. As a result, the shapes of the LUMOs are important for the chemical reactivity of the sumanene-type hexagon in the DA reaction. For other C–C bonds, small contributions of the LUMO could be found for bonds 17 and 23, and they only provide modestly exothermic products.

CONCLUSIONS

In summary, the Diels–Alder reaction to all the nonequivalent C–C bonds of C_{82} and $Sc_2C_2@C_{82}$ has been investigated to uncover their chemical reactivity. In particular, the chemical reactivity of the sumanene-type hexagon in $Sc_2C_2@C_{82}$ has also been disclosed. For C_{82} , the addition on the [5,6] bond 7 leads to the thermodynamic product, whereas the addition on the [6,6] bond 3 generates the kinetic product. In the case of $Sc_2C_2@C_{82}$, the exohedral reactivity of most bonds is reduced remarkably compared to that of the free fullerene. However, the reaction on [6,6]-type A bond 19 of the sumanene-type hexagon generates more negative reaction energy and the same energy barrier compared to the free fullerene, which results in the most favorable product under thermodynamic and kinetic conditions. Further analyses reveal that the combination of the shortest bond length, the third largest POAV, and the proper shape of LUMOs of bond 19 should contribute to its high reactivity. Overall, both the unique structure of the sumanene-type hexagon and the encapsulation of the Sc_2C_2 cluster lead to the high reactivity of bond 19 in $Sc_2C_2@C_{82}$, and the present work may stimulate further investigations on chemical reactivity of carbide clusterfullerenes.

ASSOCIATED CONTENT

Supporting Information

The Supporting Information is available free of charge on the ACS Publications website at DOI: 10.1021/acs.joc.6b00947.

Representation of the different [6,6], [5,6], and [5,5] bond types that may be present in the fullerene structures; molecular structures of C_{82} and $Sc_2C_2@C_{82}$ (side view); relative energies of 66 adducts for $Sc_2C_2@C_{82}$ in the Diels–Alder reaction at the level of M06-2X/3-21G; Cartesian coordinates of C_{82} , $Sc_2C_2@C_{82}$, and relevant structures in the Diels–Alder reaction (PDF)

AUTHOR INFORMATION

Corresponding Author

*Fax: +86 29 8266 8559. Tel: +86 29 8266 5671. E-mail: xzhao@mail.xjtu.edu.cn.

Notes

The authors declare no competing financial interest.

ACKNOWLEDGMENTS

This work has been financially supported by the National Natural Science Foundation of China (No. 21573172), the National Key Basic Research Program of China (Nos. 2011CB209404 and 2012CB720904), the Specialized Research Fund for the Doctoral Program of Higher Education of China (SRFDP No. 20130201110033), the 56th Postdoctoral Fund in China (No. 2014MS60758), and MOE Key Laboratory for Nonequilibrium Condensed Matter and Quantum Engineering. We also acknowledge special financial support from Nanotechnology Platform Program (Molecule and Material Synthesis) of the Ministry of Education, Culture, Sports, Science, and Technology (MEXT) of Japan.

REFERENCES

- (1) Akasaka, T.; Nagase, S. *Endofullerenes: A New Family of Carbon Clusters*; Kluwer Academic Publishers: Dordrecht, The Netherlands, 2002.

- (2) Heath, J. R.; O'Brien, S. C.; Zhang, Q.; Liu, Y.; Curl, R. F.; Tittel, F. K.; Smalley, R. E. *J. Am. Chem. Soc.* **1985**, *107*, 7779.
- (3) Solomon, S. *Nature* **1990**, *347*, 347.
- (4) Wilson, L. J.; Cagle, D. W.; Thrash, T. P.; Kennel, S. J.; Mirzadeh, S.; Alford, J. M.; Ehrhardt, G. J. *Coord. Chem. Rev.* **1999**, *192*, 199.
- (5) Shinohara, H. *Rep. Prog. Phys.* **2000**, *63*, 843.
- (6) Popov, A. A.; Yang, S.; Dunsch, L. *Chem. Rev.* **2013**, *113*, 5989.
- (7) Chaur, M. N.; Melin, F.; Ortiz, A. L.; Echegoyen, L. *Angew. Chem., Int. Ed.* **2009**, *48*, 7514.
- (8) Martin, N. *Chem. Commun.* **2006**, 2093.
- (9) Dunsch, L.; Yang, S. *Small* **2007**, *3*, 1298.
- (10) *Chemistry of Nanocarbons*; Akasaka, T., Wudl, F., Nagase, S., Eds.; Wiley: New York, 2010.
- (11) Tan, Y. Z.; Xie, S. Y.; Huang, R. B.; Zheng, L. S. *Nat. Chem.* **2009**, *1*, 450.
- (12) Osuna, S.; Swart, M.; Sola, M. *Phys. Chem. Chem. Phys.* **2011**, *13*, 3585.
- (13) Yang, S.; Liu, F.; Chen, C.; Jiao, M.; Wei, T. *Chem. Commun.* **2011**, *47*, 11822.
- (14) Lu, X.; Feng, L.; Akasaka, T.; Nagase, S. *Chem. Soc. Rev.* **2012**, *41*, 7723.
- (15) Lu, X.; Akasaka, T.; Nagase, S. *Chem. Commun.* **2011**, *47*, 5942.
- (16) Lu, X.; Bao, L.; Akasaka, T.; Nagase, S. *Chem. Commun.* **2014**, *50*, 14701.
- (17) Stevenson, S.; Rice, G.; Glass, T.; Harich, K.; Cromer, F.; Jordan, M. R.; Craft, J.; Hadju, E.; Bible, R.; Olmstead, M. M.; Maitra, K.; Fisher, A. J.; Balch, A. L.; Dorn, H. C. *Nature* **1999**, *401*, 55.
- (18) Maeda, Y.; Tsuchiya, T.; Lu, X.; Takano, Y.; Akasaka, T.; Nagase, S. *Nanoscale* **2011**, *3*, 2421.
- (19) Yang, T.; Nagase, S.; Akasaka, T.; Poblet, J. M.; Houk, K. N.; Ehara, M.; Zhao, X. *J. Am. Chem. Soc.* **2015**, *137*, 6820.
- (20) Martínez, J. P.; Garcia-Borràs, M.; Osuna, S.; Poater, J.; Bickelhaupt, F. M.; Solà, M. *Chem. - Eur. J.* **2016**, *22*, 5953.
- (21) Li, F.-F.; Pinzon, J. R.; Mercado, B. Q.; Olmstead, M. M.; Balch, A. L.; Echegoyen, L. *J. Am. Chem. Soc.* **2011**, *133*, 1563.
- (22) Feng, L.; Wakahara, T.; Nakahodo, T.; Tsuchiya, T.; Piao, Q.; Maeda, Y.; Lian, Y.; Akasaka, T.; Horn, E.; Yoza, K.; Kato, T.; Mizorogi, N.; Nagase, S. *Chem. - Eur. J.* **2006**, *12*, 5578.
- (23) Feng, L.; Nakahodo, T.; Wakahara, T.; Tsuchiya, T.; Maeda, Y.; Akasaka, T.; Kato, T.; Horn, E.; Yoza, K.; Mizorogi, N.; Nagase, S. *J. Am. Chem. Soc.* **2005**, *127*, 17136.
- (24) Lu, X.; Akasaka, T.; Nagase, S. *Acc. Chem. Res.* **2013**, *46*, 1627.
- (25) Garcia-Borràs, M.; Osuna, S.; Luis, J. M.; Swart, M.; Solà, M. *Chem. - Eur. J.* **2013**, *19*, 14931.
- (26) Garcia-Borràs, M.; Osuna, S.; Luis, J. M.; Swart, M.; Solà, M. *Chem. - Eur. J.* **2012**, *18*, 7141.
- (27) Osuna, S.; Swart, M.; Campanera, J. M.; Poblet, J. M.; Solà, M. *J. Am. Chem. Soc.* **2008**, *130*, 6206.
- (28) Osuna, S.; Swart, M.; Solà, M. *J. Am. Chem. Soc.* **2009**, *131*, 129.
- (29) Iiduka, Y.; Wakahara, T.; Nakajima, K.; Nakahodo, T.; Tsuchiya, T.; Maeda, Y.; Akasaka, T.; Yoza, K.; Liu, M. T. H.; Mizorogi, N.; Nagase, S. *Angew. Chem., Int. Ed.* **2007**, *46*, 5562.
- (30) Chen, C. H.; Yeh, W. Y.; Liu, Y. H.; Lee, G. H. *Angew. Chem., Int. Ed.* **2012**, *51*, 13046.
- (31) Chen, C. H.; Lin, D. Y.; Yeh, W. Y. *Chem. - Eur. J.* **2014**, *20*, 5768.
- (32) Cai, W.; Chen, M.; Bao, L.; Xie, Y.; Akasaka, T.; Lu, X. *Chem. - Eur. J.* **2015**, *21*, 3449.
- (33) Dang, J. S.; Wang, W. W.; Zhao, X.; Nagase, S. *Org. Lett.* **2014**, *16*, 170.
- (34) Dang, J. S.; Wang, W. W.; Nagase, S.; Zhao, X. *J. Phys. Chem. C* **2013**, *117*, 12882.
- (35) Zhao, Y.; Schultz, N. E.; Truhlar, D. G. *J. Chem. Theory Comput.* **2006**, *2*, 364.
- (36) Hariharan, P. C.; Pople, J. A. *Theoret. Chim. Acta* **1973**, *28*, 213.
- (37) Zhao, Y.; Truhlar, D. G. *Theor. Chem. Acc.* **2008**, *120*, 215.
- (38) Fukui, K. *J. Phys. Chem.* **1970**, *74*, 4161.
- (39) Gonzalez, C.; Schlegel, H. B. *J. Chem. Phys.* **1989**, *90*, 2154.
- (40) Gonzalez, C.; Schlegel, H. B. *J. Phys. Chem.* **1990**, *94*, 5523.
- (41) Frisch, M. J.; Trucks, G. W.; Schlegel, H. B.; Scuseria, G. E.; Robb, M. A.; Cheeseman, J. R.; Scalmani, G.; Barone, V.; Mennucci, B.; Petersson, G. A.; Nakatsuji, H.; Caricato, M.; Li, X.; Hratchian, H. P.; Izmaylov, A. F.; Bloino, J.; Zheng, G.; Sonnenberg, J. L.; Hada, M.; Ehara, M.; Toyota, K.; Fukuda, R.; Hasegawa, J.; Ishida, M.; Nakajima, T.; Honda, Y.; Kitao, O.; Nakai, H.; Vreven, T.; Montgomery, J. A., Jr.; Peralta, J. E.; Ogliaro, F.; Bearpark, M.; Heyd, J. J.; Brothers, E.; Kudin, K. N.; Staroverov, V. N.; Kobayashi, R.; Normand, J.; Raghavachari, K.; Rendell, A. J.; Burant, C.; Iyengar, S. S.; Tomasi, J.; Cossi, M.; Rega, N.; Millam, J. M.; Klene, M.; Knox, J. E.; Cross, J. B.; Bakken, V.; Adamo, C.; Jaramillo, J.; Gomperts, R.; Stratmann, R. E.; Yazyev, O.; Austin, A. J.; Cammi, R.; Pomelli, C.; Ochterski, J. W.; Martin, R. L.; Morokuma, K.; Zakrzewski, V. G.; Voth, G. A.; Salvador, P.; Dannenberg, J. J.; Dapprich, S.; Daniels, A. D.; Farkas, O.; Foresman, J. B.; Ortiz, J. V.; Cioslowski, J.; Fox, D. J. *Gaussian 09*, revision A.01; Gaussian, Inc.: Wallingford, CT, 2009.
- (42) Campanera, J. M.; Bo, C.; Poblet, J. M. *J. Org. Chem.* **2006**, *71*, 46.
- (43) Osuna, S.; Valencia, R.; Rodriguez-Fortea, A.; Swart, M.; Solà, M.; Poblet, J. M. *Chem. - Eur. J.* **2012**, *18*, 8944.
- (44) Zhao, P.; Dang, J. S.; Zhao, X. *Phys. Chem. Chem. Phys.* **2016**, *18*, 9709.
- (45) Yang, T.; Zhao, X.; Nagase, S.; Akasaka, T. *Chem. - Asian J.* **2014**, *9*, 2604.
- (46) Haddon, R. C. *Acc. Chem. Res.* **1988**, *21*, 243.
- (47) Woodward, R. B.; Hoffmann, R. *Angew. Chem., Int. Ed. Engl.* **1969**, *8*, 781; *Angew. Chem.* **1969**, *81*, 797.
- (48) Fukui, K. *Molecular Orbitals in Chemistry, Physics and Biology*; Lowdin, P. O., Pullman, B., Eds.; Academic Press: New York, 1964; p 513.